Chapter 2. Theory

In this Chapter, basic information about some geochemical and isotopic parameters and their behaviour in geo-hydrological environment is provided. Principles of various groundwater dating methods, such as ^{14}C, ^{4}He and $^{4}He/^{222}Rn$ (employed in this study) and CFCs (for which a new laboratory was set up), are also discussed.

2.1 Helium

Helium (^{4}He) is the second most abundant element in the known Universe after hydrogen and constitutes 23% of the elemental mass of the Universe. It is the second lightest element in the periodic table after hydrogen. It is a colourless, odourless, non-toxic, and virtually inert mono-atomic gas. It was discovered in 1868 by J. Norman Lockyear in the spectrum of a solar eclipse. The fact sheet of helium is given in the Table 2.1.

Table 2.1 The fact sheet of Helium (compiled from CRC handbook)

Name (Symbol)	Helium (He)
Atomic Number	2
Atomic mass	4.002602 g/mol
Chemical series	Noble gases
Group, period, block	18, 1, s
Electronic configuration	$1s^2$
Electrons per shell	2
Stable isotopes (Natural abundance)	^{4}He (99.999863%), ^{3}He (0.000137%)
Radioactive isotopes	^{5}He ,^{6}He , ^{7}He, ^{8}He, ^{9}He, ^{10}He
Atmospheric concentration	5.3 parts per million (ppm) by volume
Diffusivity in water at 25^{0}C	$7.78x10^{-5}$ cm^2s^{-1}
Recoil path length	30–100 μm

Although there are eight known isotopes of helium, only two isotopes namely ^{4}He (2 protons and 2 neutrons) and ^{3}He (2 protons and 1 neutron) are stable. The remaining six isotopes are all radioactive and extremely short lived. The isotopic abundance of helium, however, varies greatly depending on its origin. On earth, helium is produced by the radioactive decay of much heavier elements such as Uranium and Thorium. The alpha particles produced during radioactive alpha-decay are nothing but fully ionised ^{4}He nuclei. In the ^{238}U, ^{235}U and ^{232}Th series, the decay chains yield respectively 8, 7 and 6 atoms of ^{4}He (Figure 2.1).

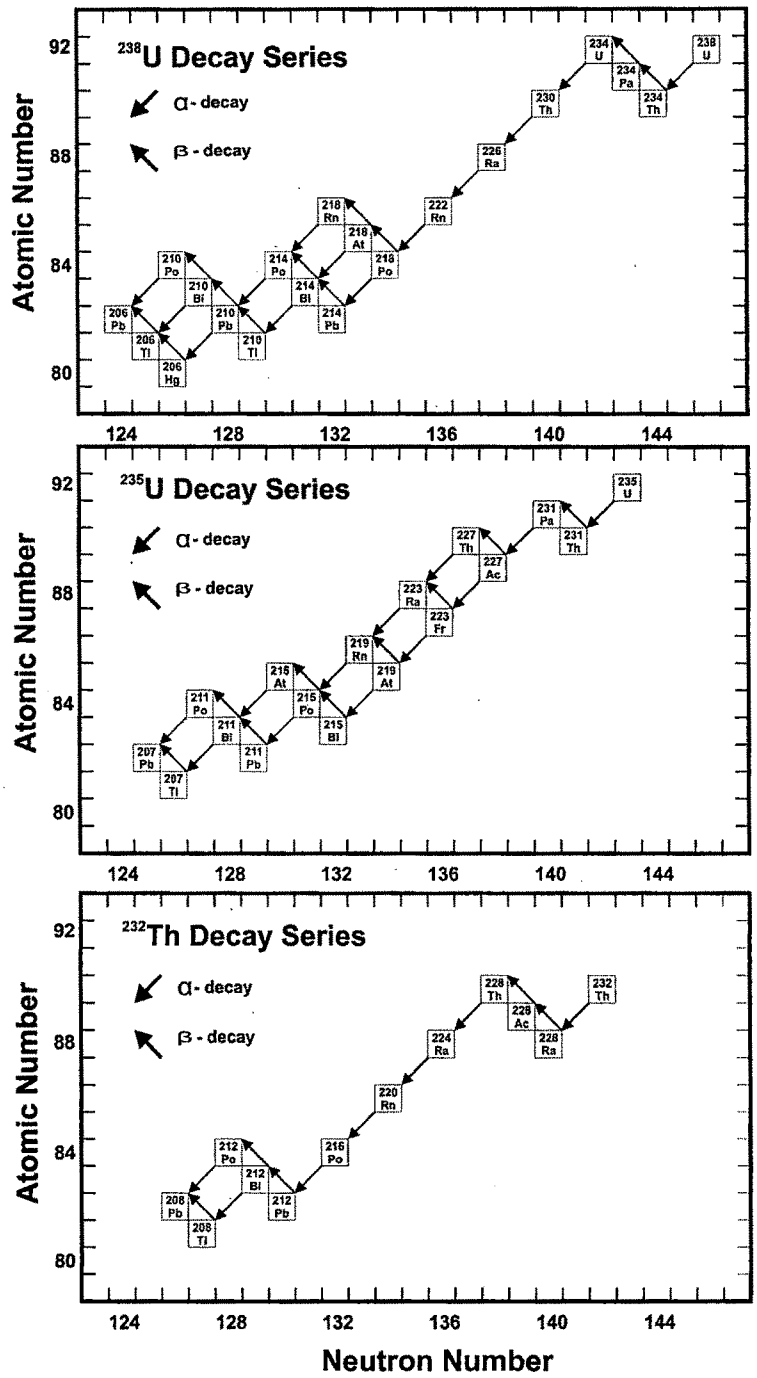

Figure 2.1 Radioactive decay series of Uranium and Thorium showing production of α particles (the helium nucleus) and the ^{222}Rn. Note that 8, 7 and 6 helium atoms are produced in the decay chains of ^{238}U, ^{235}U and ^{232}Th respectively. ^{222}Rn is produced in the decay chain of ^{238}U.

Helium so produced is released from grains by their etching, dissolution and fracturing and by alpha recoil and then exhaled into the atmosphere by diffusion and

temperature variations. Since helium is produced in rocks and soils within earth and escapes to outer space from the top of the atmosphere due to its inertness and low mass, its concentration shows a gradient decreasing towards the ground-atmosphere interface. In the Earth's atmosphere, the concentration of helium is only ~5.3 parts per million (ppm) by volume.

Water in solubility equilibrium with the atmosphere usually shows low concentrations of helium because of its low solubility (~1%) and low atmospheric concentration. In ground waters, however, dissolved helium can be high due to its radioactive production and release from earth materials. Since its diffusivity in water is low (7.78×10^{-5} cm^2s^{-1} at 25^0C; CRC handbook), it gets trapped in groundwater and collects additional radiogenic helium from the aquifer matrix while moving through it till groundwater comes in contact with atmosphere. This provides the basis for groundwater dating by the helium method using the knowledge of helium production rate in the aquifer matrix from its uranium and thorium content (Fröhlich and Gellermann, 1987; Torgersen, 1980; 1992; Mazor and Bosch, 1992; Clark et al, 1998; Castro et al, 2000). Presence of fractures and fissures, particularly in hard rocks, provide preferential pathways for migration of radiogenic helium from the subsurface interconnected spaces between the grains. Therefore, depending on the collection volume of a particular fracture or fissure, helium concentration in the groundwater residing in the particular fracture zone can be significantly higher than its production from the rock volume in contact with groundwater. This then forms the basis of delineating the deep structural zones (Kulongoski et al, 2005; Kulongoski et al, 2003; Gupta and Deshpande, 2003a; Gülec et al, 1987; Minisalle et al, 2000; Filippo et al, 1999). Moreover during and just before earthquakes, enhancement in helium concentration in some ground waters has been noticed (Reimer, 1984; Barsokov et al, 1984; Rao et al, 1994). This is possibly due to rock dilation and fracturing during incipient fault movements and forms the basis for using helium monitoring as a tool for earthquake prediction. The important point to be noticed is that all the radiogenic helium may not be released from the rock matrix in the normal course giving a release factor of less than unity. This may have implications for groundwater dating using helium and helium/radon dating as discussed subsequently (see Sections 2.6.2 and 2.6.3). When the groundwater has dissolved helium in excess of atmospheric equilibration value, the groundwater is referred to as having 'helium anomaly' or 'excess helium'. Ground waters may have 'excess helium' also due to other factors, viz., (i) occurrence of uranium mineralization within a particular aquifer zone or in its vicinity – forming basis for radioactive mineral exploration (Reimer, 1976); and (ii) occurrence of natural gas reservoir, below the aquifer system, which can have high concentration of helium – forming basis for petroleum exploration using helium surveys (Jones and Drozd,

1983; Weismann, 1980). In addition, depending on the physical nature of capillary fringe zone just above the saturated zone, air bubbles ca be entrapped and transported into the saturated zone. The air bubbles can also be entrapped by rapid rise in the water table due to occasional heavy rainfall in semi arid regions. Entrapment and subsequent dissolution of such air bubbles into the groundwater introduces excess-air and consequently all its components including helium. This contributes additional helium to groundwater over and above atmospheric equilibration value (Heaton, 1981; Heaton and Vogel, 1981; Andrews et al, 1985).

2.2 Radon

Radon (Rn) is a chemically inert, radioactive noble gas formed by the disintegration of Ra (radium) in the decay chains of Uranium and Thorium (Figure 2.1). It was discovered in 1900 by Friedrich Ernst Dorn. There are twenty known radioactive isotopes of radon but it does not have any stable isotope. Among its isotopes, ^{222}Rn formed by decay of ^{226}Ra (in the ^{238}U decay series; Figure 2.1), has the longest half-life of 3.8235 days and decays to ^{218}Po (Polonium) by emitting an α–particle. The fact sheet of Radon is given in the Table 2.2.

Table 2.2 The fact sheet of Radon (compiled from CRC handbook)

Name (Symbol)	Radon (Rn)
Atomic Number	86
Atomic mass	222 g/mol
Chemical series	Noble gases
Group, period, block	18, 6, p
Electronic configuration	[Xe] $4f^{14}$ $5d^{10}$ $6s^2$ $6p^6$
Electrons per shell	2, 8, 18, 32, 18, 8
Stable isotopes	None
Radioactive isotopes	^{195} Rn to ^{228} Rn (only 20 natural)
Natural abundance	^{222}Rn (100%)
Atmospheric activity	~$7x10^{-4}$dpm/l
Diffusivity in water at 25^0C	1.33x 10^{-5} cm^2s^{-1}
Recoil path length	~0.05 μm

Natural radon concentration in the earth's atmosphere is very low (1 in 10^{21} molecules of air) due to its radioactive decay though it has been shown to accumulate in the air if there is a meteorological inversion. The natural waters in equilibrium with the atmosphere has low concentration of ~$7x10^{-4}$ dpm/l (Gupta et al, 2002).

Ground waters can have higher concentration of ^{222}Rn due to release from subsurface production. Due to its diffusion into the atmosphere, radon content of

unsaturated zone, in common with other inert gases, is lower than in the saturated zone. The mobility of radon in ground waters is to some extent linked to its parent radium, which is particle and salinity sensitive (Krishnaswami et al, 1991).

As with helium, the faults and fractures in the crust act as preferential pathways for migration of radon. Unlike helium that can go on accumulating in stationary or confined ground waters (Gupta et al, 2002), radon is expected to be in a steady state between production, decay and mobilisation from rock/soil matrix. Though, during and for a short time following any disturbance, such as an earthquake, the steady state conditions may not prevail. Similar to helium anomalies, the radon anomalies have also been used as seismic precursors (Shapiro, 1981; Virk et al, 2001), delineation of active fracture zones (Reddy et al, 2006), radioactive mineral exploration (Jones and Drozd, 1983; Weismann, 1980) and in groundwater dating using helium/radon ratio (Gupta et al, 2002; Agarwal et al, 2006). In this last application due to the fact that both radiogenic gases are produced from the decay of ^{238}U, their ratio is independent of uranium concentration (Torgersen, 1980).

Radon is one of the heaviest gases at room temperatures and can accumulate in buildings, and drinking water, and cause lung cancer (BEIR, 1999). Therefore, it is considered to be a health hazard. It is probably the most significant contaminant in indoor air quality worldwide.

2.3 Fluoride

In aqueous solution, element fluorine (F) commonly occurs as the fluoride ion (F^-). In ground waters fluoride is one of the most important environmental pollutant due to natural and/or anthropogenic factors. Pure fluorine (F_2) is a corrosive pale yellow gas that is a powerful oxidizing agent. It is the most reactive and electronegative of all the elements, and readily forms compounds with most other elements including noble gases. The fact sheet of fluorine is presented in Table 2.3.

The ill effects of excessive fluorine/ fluoride ingestion on human health have been extensively studied (WHO, 1970; 1984; Gupta and Deshpande, 1998; Luke, 1997; Zero et al, 1992). The occurrence and development of endemic fluorosis has its roots in the high fluoride content in water, air and soil, of which water is perhaps the major contributor. Bureau of Indian Standards (BIS, 1990) has suggested the permissible limit of fluoride in drinking water as 1 part per million (ppm), which is lower then the WHO (1984) drinking water limit of 1.5 ppm. Gupta and Deshpande (1998) have described the hazardous effects on human and cattle health from ingestion of excessive fluoride in the NGC region where it was observed that ingestion of excessive fluoride has adverse effect on teeth and bones (known as dental and skeletal fluorosis).

Table 2.3 The fact sheet of Fluorine (compiled from CRC handbook)

Name (Symbol)	Fluorine (F)
Atomic Number	9
Atomic mass	18.9984032 g/mol
Chemical series	Halogens
Group, period, block	17, 2, p
Electronic configuration	$1s^2\ 2s^2\ 2p^5$
Electrons per shell	2, 7
Stable isotopes	^{19}F
Radioactive isotopes	^{14}F to ^{31}F (although there are many radioactive isotopes of fluorine, they all have such a short half-life that fluorine is generally considered mono-isotopic element.
Permissible limit in drinking water	1.5 ppm (Parts per Million or mg/l); WHO, 1984. 1.0 ppm; BIS, 1990.

The normal fluoride content in the atmospheric air is reported between 0.01–0.4 $\mu g/m^3$. However, in industrial areas, it is known to range from 5 to 111 $\mu g/m^3$ (Oelschläger, 1965; Bowen, 1966). Average fluoride content of precipitation varies from almost nil to 0.089 mg/l with as high as 1 mg/l (Gmelin, 1959; Sugawara, 1967) in industrial areas. The fluoride content of rivers also varies greatly depending on the fluoide content of effluent discharges of groundwater feeding the stream and on the amount of precipitation and runoff. The fluoride content in surface water is generally higher during dry period due to evaporative concentration (Deshmukh et al, 1995b). The mean concentration of fluoride in ocean waters ranges from 0.03 to 1.35 mg/l and is seen to increase with depth in many cases (Bewers, 1971; Riley, 1965). The groundwaters, particularly in the arid/ semiarid regions throughout the globe are known to have high fluoride concentration (Handa, 1977).

The fluoride content of groundwater greatly depends on the type of soil/rocks/aquifer it comes in contact with. There are more than 150 fluorine bearing minerals in the form of silicates, halides and phosphates (Strunz, 1970; Wedepohl, 1974). Fluorite (CaF_2) is the most widely distributed fluorine bearing mineral in nature while fluorapatite ($Ca_5\ F\ (PO_4)_3$) is a very common member of the immiscible phase generated during early differentiation of mafic and ultramafic magmas, forming apatite-magnetite rocks. In advanced stage of differentiation, fluorine is enriched into the residuum and therefore rocks like granitoids or pegmatites have very high content of apatite resulting in average fluorine content of up to 2.97 % (by weight) in these rocks. In sedimentary rocks, in addition to fluorite and fluorapatite in clastic component, clay sized minerals like micas (muscovite, biotite, phlogopite, zinnwaldite and lepidolite) and clay minerals

(montrmorillonite, illite and kaolinite) have high content of fluorine due to replacement of OH^- by F^- or due to admixture of skeletal debris in which hydroxyl bonds are replaced by fluorine in the hydoxy-apatite structure (Carpenter, 1969). Out of the total fluorine content of the clay sized particles, 80 to 90 % is hosted in the micaceous minerals and remainder is associated with clay minerals (Koritnig, 1951). The fluorine content of soils depends mainly on the rocks from which they have been derived and the climatic regime in which the soil is formed. However, in warm and humid climate decomposition of organic remains can be principal source of fluorine. The average fluorine content in the soil ranges between 90 to 980 ppm (Fleischer and Robinson, 1963). The leaching of fluoride from soils and aquifer matrix into groundwater involves adsorption-desorption and dissolution-precipitation processes. Since the solubility of fluorite and fluorapatite is very low in natural waters (Deshmukh et al, 1995a), in the leaching process it is dissolved slowly by the circulating water but fluoride from mica is leached out rapidly. However, on account of the ionic strength of complex forming ions, solubility of fluorite can be drastically modified. Calcium and sulphate ions significantly lower the fluorite solubility in natural waters, often causing precipitation of fluorite (Handa, 1977; Perel'man, 1977; Deshmukh et al, 1993). The distribution of Ca and F in groundwater is therefore, antipathic (Handa, 1977; Deshmukh et al, 1995a; Dev et al, 1995; Srivastava et al, 1996). Fluorine from the clay minerals is readily desorbed in the alkaline environment. Fluoride to hydroxyl ion exchange in clay minerals depends upon concentration of fluoride ion and pH of circulating water (Hubner, 1969 a; b). Thus, solubility of fluorine bearing minerals is governed by various parameters like pH, alkalinity, ionic strength, calcium and sulphate ion concentration etc.

It is seen from the global map (Figure 2.2) of endemic fluorosis reproduced from UNICEF website (http://www.unicef.org/programme/wes/info/fl_map.gif) that most of the fluoride affected regions have arid to semiarid climate. In India, fluoride rich ground waters are found in the arid parts, especially Rajasthan, Gujarat and interior parts of the southern peninsula characterised by episodic rainfall separated by extended dry periods (Agrawal et al. 1997; Vasavada, 1998; Jacks et al. 1993). Fluoride poisoning is also reported from the arid climatic regime (Yong and Hua, 1991) in North China.

The fluoride content of thermal springs can increase with temperature due to increased rock-water interaction at elevated temperature (Chandrasekharam and Antu, 1995) and /or scavenging from the large volume during hydrothermal circulation (Minissale et al, 2000; Gupta and Deshpande 2003a) but this is not observed as a rule. There are thermal springs with as low concentraion of fluoride as <0.15 mg/l and as high concentration as 55.4 mg/l (Gmelin, 1959; Sugawara, 1967).

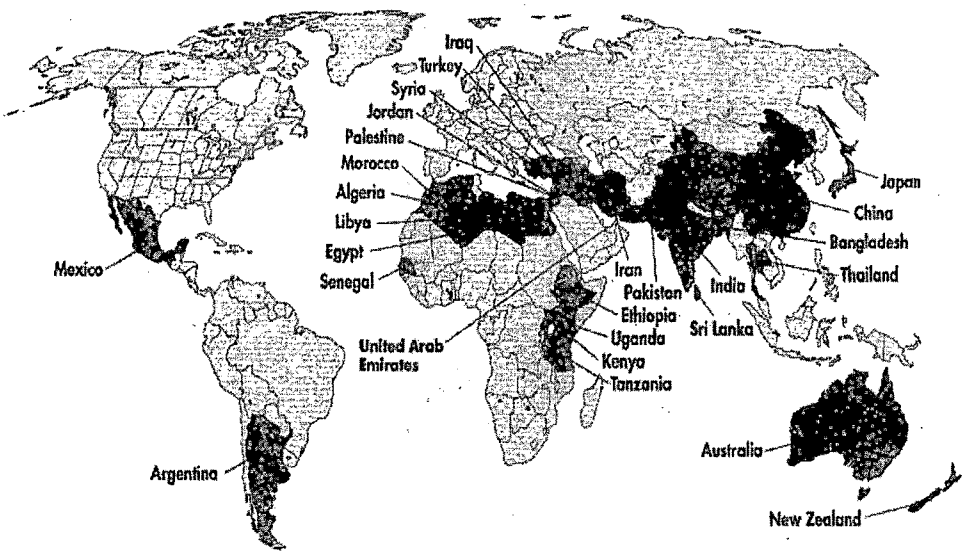

Figure 2.2 Global distribution of endemic fluorosis. Note that the most affected areas are in arid/ semiarid regions. Source-http://www.unicef.org/programme/wes/info/fl_map.gif.

2.4 Stable Isotopes of Oxygen and Hydrogen

Among various isotopes used as tracers in hydrology, stable isotopes of oxygen (^{18}O) and hydrogen (^{2}H, also known as deuterium; D) are the most important. Since these form integral parts of water molecules; these are ideally suited to follow the movement of water throughout the hydrological cycle. The basic fact sheet of these isotopes is given in Table 2.4.

In hydrological parlance, the two isotopes are also referred to as water isotopes. Importance and applications of water isotopes to hydrological studies have been discussed at length and demonstrated in several parts of the world (Dincer et al, 1974; Salati et al, 1979; Gonfiantini, 1986; Gat and Matsui, 1991; Rozanski et al, 1993; Clark and Fritz, 1997; Kendall and Mcdonnell, 1998; Araguas-Araguas et al, 1998). Several Indian case studies have been reported over the last few decades (Kumar et al, 1982; Bhattacharya et al, 1985; Das et al, 1988; Krishnamurty and Bhattacharya, 1991; Datta et al, 1991; Chandrasekharan et al, 1992; Navada et al, 1991, 1993; Datta et al, 1994,1996; Yadava, 1997; Sukhija et al, 1998; Bhattacharya et al, 2003; Deshpande et al, 2003; Shivanna et al, 2004) and in recent years by Gupta and Deshpande (2003 c; 2005 a, b, c) and Gupta et al (2005b).

Table 2.4 The fact sheet of Oxygen and Hydrogen (compiled from CRC handbook)

Name (Symbol)	Oxygen (O)	Hydrogen (H)
Atomic number	8	1
Atomic Mass	15.9994 g/mol	1.00794 g/mol
Chemical Series	Non-metals, chalcogens	non-metals
Group, period, block	16, 2, p	1, 1, s
Electronic configuration	$1s^2\ 2s^2\ 2p^4$	$1s^1$
Electrons per shell		1
Stable isotopes (Natural Abundance)	^{16}O (99.76%) ^{17}O (0.038%) ^{18}O (0.21%)	^{1}H (99.985%) ^{2}H (0.015%)
Radioactive isotopes	Fourteen isotopes from ^{12}O to ^{28}O excepting ^{16}O, ^{17}O and ^{18}O. All radioactive isotopes have half-life less than 3 minutes	^{3}H (tritium) With half-life of 12.3 years. ^{3}H beta-decays to ^{3}He.

Isotopic compositions are normally expressed in δ–notation, as deviations of heavy to light isotopic ratios relative to an international standard of known composition, in units of parts per thousand or per mil (denoted as ‰). The δ values are calculated as:

$$\delta\ (\text{in } ‰) = (R_x / R_s - 1) \times 1000 \qquad \text{Eq. (2.1)}$$

where R_x and R_s denote the ratio of heavy to light isotope (e.g. $^{18}O/^{16}O$ or D/H) in the sample and standard respectively. Both, δD and $\delta^{18}O$ values, are normally reported relative to SMOW (Standard Mean Ocean Water; Craig, 1961a) or the equivalent VSMOW (Vienna-SMOW; Gonfiantini, 1978) standard.

Isotopic fractionation occurs mainly by (i) equilibrium isotopic exchange reactions and (ii) kinetic processes. Equilibrium exchange reactions involve redistribution of the isotopes between the products and reactants (or the two phases during phase change) in contact with each other. As a 'rule of thumb', among different phases of the same compound (e.g. H_2O), the denser the material, the more it tends to be enriched in the heavier isotope (D and ^{18}O).

In systems out of equilibrium, forward and backward reaction rates are not identical, and isotope reactions become unidirectional, e.g., when reaction products are physically isolated from the reactants. Such reactions are called kinetic. A third reaction

type where fractionation of isotopes occurs is the diffusion of atoms or molecules across a concentration gradient. This can be diffusion within another medium or diffusion of a gas into vacuum. In this case fractionation arises from the difference in diffusive velocities of isotopic molecular species.

The isotope fractionation is expressed by a fractionation factor (α), which is the ratio of the isotope ratios for reactant and product ($\alpha = R_{reactant}/R_{product}$). For example, in case of water→ vapour system, the fractionation factor is given by;

$$\alpha^{18}O_{(water \rightarrow vapour)} = \left(^{18}O/_{16}O\right)_{water} \Big/ \left(^{18}O/_{16}O\right)_{vapour}$$

Eq. (2.2)

Craig (1961b) showed that in spite of the great complexity in different components of the hydrological cycle, $\delta^{18}O$ and δD in fresh waters correlate on a global scale. Craig's global meteoric water line or GMWL defines the relationship between $\delta^{18}O$ and δD in global precipitation as:

$$\delta D = 8 \times \delta^{18}O + 10 \quad (‰ \text{ SMOW})$$

Eq. (2.3)

This equation indicates that the isotopic composition of meteoric waters behave in fairly predictable fashion. The GMWL is average of many local or regional meteoric water lines, which may somewhat differ from each other due to varying climatic and geographic parameters. A Local Meteoric Water Line (LMWL) can differ from global line in both slope and deuterium intercept. Nonetheless, GMWL provides a reference for interpreting the hydrological processes and provenance of different water masses.

Improving the precision of the Craig's GMWL, Rozanski et al (1993) compiled the precipitation isotope data from 219 stations of the IAEA/WMO operated Global Network for Isotopes in Precipitation (GNIP). This refined relationship between ^{18}O and D in global precipitation (Figure 2.3) is given by:

$$\delta D = 8.17(\pm 0.07) \times \delta^{18}O + 11.27(\pm 0.65) \quad (‰ \text{ VSMOW})$$

Eq. (2.4)

The evolution of $\delta^{18}O$ and δD values of meteoric waters begins with evaporation from the oceans, where the rate of evaporation controls the water - vapour exchange and hence the degree of isotopic equilibrium. Increased rates of evaporation impart a kinetic or non-equilibrium isotope effect to the vapour. Kinetic effects are influenced by

surface temperature, wind speed (shear at water surface), salinity and, most importantly humidity. At lower values of humidity, evaporation becomes an increasingly non-equilibrium process.

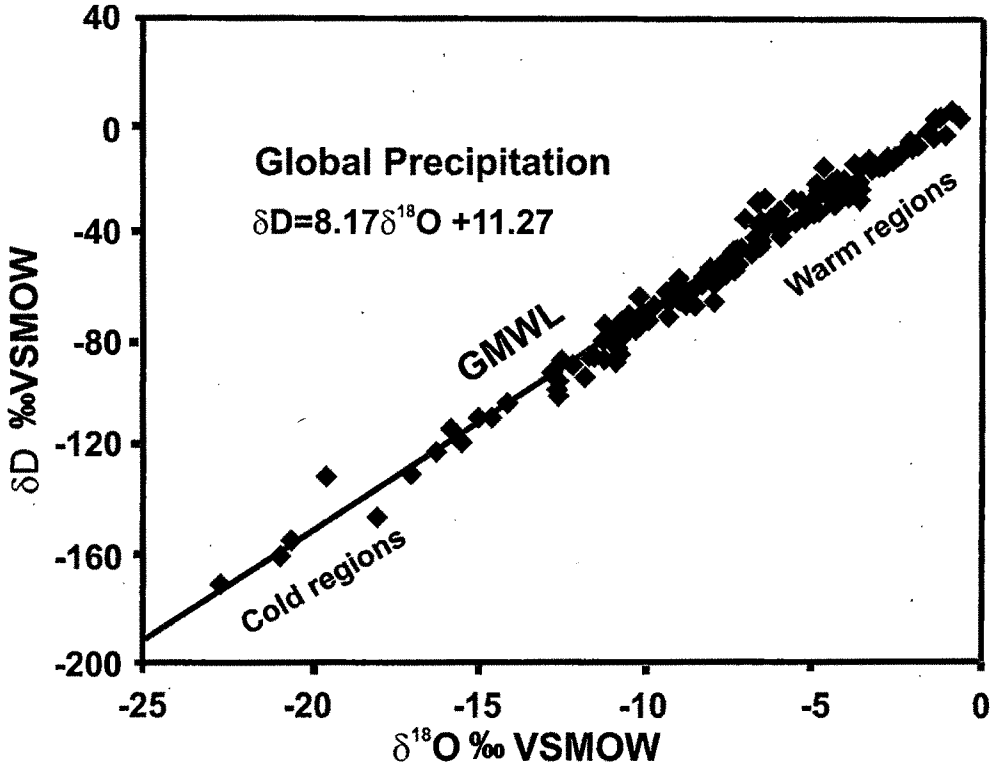

Figure 2.3 The linear regression line between $\delta^{18}O$ and δD of global precipitation samples. Data are weighted average annual values for precipitation monitored at 219 stations of IAEA/WMO global network. Redrawn from Rozanski et al (1993).

The most accepted model for non-equilibrium evaporation from a water body involves diffusion of water vapour across a hypothetical microns thin boundary layer (bl) over the liquid water interface. The boundary layer has virtually 100% water saturation. This layer is in isotopic equilibrium with the underlying water column. Between the boundary layer and the mixed atmosphere above is a transition zone through which water vapour is transported in both directions by molecular diffusion. It is within the transition zone that non-equilibrium fractionation arises due to the fact that diffusivity of $^{1}H_2{}^{16}O$ in air is greater than that of $^{2}H^{1}H^{16}O$ or $H_2{}^{18}O$. The additional isotopic enrichment ($\Delta\varepsilon$) of evaporating water due to kinetic fractionation at relative humidity (h; fractional) is approximated by the following two empirical relationships (Gonfiantini, 1986) that ignore all other controlling factors except the humidity:

$$\Delta\varepsilon^{18}O_{bl\text{-}v} = 14.2 \times (1 - h)\ ‰$$

Eq. (2.5)

$$\Delta\varepsilon^{2}H_{bl\text{-}v} = 12.5 \times (1 - h)\ ‰$$

Eq. (2.6)

It is seen from the above equations that relative magnitude of kinetic fractionation for oxygen isotopes is significantly higher than that for hydrogen isotopes. The total enrichment between water column and open air is the sum of the enrichment factor for equilibrium water vapour exchange ($\varepsilon_{l\rightarrow v}$) and the kinetic factor ($\Delta\varepsilon_{bl\text{-}v}$). For ^{18}O, this would be:

$$\delta^{18}O_l - \delta^{18}O_v = \varepsilon^{18}O_{l\rightarrow bl} + \Delta\varepsilon^{18}O_{bl\rightarrow v}$$

Eq. (2.7)

Because the boundary layer is at 100% saturation, $\varepsilon^{18}O_{l\rightarrow bl}$ corresponds to equilibrium fractionation in water→vapour system. This calculation represents the enrichment of water with respect to vapour. The depletion in vapour with respect to water is the negative enrichment. Under conditions of 100% humidity (h = 1), the vapour is in isotopic equilibrium with seawater ($\Delta\varepsilon^{18}O_{bl\text{-}v} = 0$). When humidity is low (e.g., h = 0.5) the vapour is strongly depleted in ^{18}O compared to D. The global atmospheric vapour forms with an average humidity around 85% (h = 0.85). That is why the Craig's GMWL has deuterium intercept of 10 ‰.

Thus, formation of atmospheric vapour masses is a non-equilibrium process due to effects of lower than saturation humidity. However, the reverse process – condensation to form clouds and precipitation – takes place in an intimate mixture of vapour and water droplets with near saturation humidity so that equilibrium fractionation between vapour and water is easily achieved. As a result isotopic evolution of precipitation during rainout is largely controlled by temperature. Because of this, the slope of GMWL (8) is largely in agreement with that given by the ratio of equilibrium fractionation factors for D and ^{18}O.

$$S \approx \frac{10^3 \ln\alpha D_{v\rightarrow l}}{10^3 \ln\alpha^{18}O_{v\rightarrow l}} = 8.2 \text{ at } 25°C$$

Eq. (2.8)

However, the slopes of various LMWLs vary from 9.2 to 8.0 with average temperature of condensation between 0 to 30°C. It is thus seen that the relationship between ^{18}O and D in meteoric waters arises from a combination of non-equilibrium

fractionation from the ocean surface (at ~85% humidity) and equilibrium condensation from the vapour mass. However, during rainout, further partitioning of ^{18}O and D between different regions is governed by the Rayleigh distillation equation.

As an air mass moves from its vapour source area along a trajectory and over continents, it cools and loses its water content through the rainout process. During rainout, ^{18}O and D in vapour and the condensing phases (rain or snow), within the cloud, partition through equilibrium fractionation. But along the trajectory, as each rainout removes the vapour mass, the heavy isotopes from the vapour are preferrentially removed so that remaining vapour becomes progressively depleted in ^{18}O and D. Whereas each rainout gives isotopically enriched rain (or snow) with respect to its immediate parent vapour. It will, however, be depleted with respect to earlier rainiout, because the vapour from which it formed was isotopically depleted with respect to the vapour of the earlier rainout. One can model this isotope evolution during rainout according to Rayleigh distillation equation as below.

$$R_V = R_{V0}\, f^{(\alpha - 1)}$$

Eq. (2.9)

Because $R_l / R_v = \alpha = R_{l0} / R_{v0}$; this equataion can also be written in terms of liquid water, i.e.

$$R_l = R_{l0}\, f^{(\alpha - 1)}$$

Eq. (2.10)

In above equation, R_{V0} is initial isotope ratio ($^{18}O/^{16}O$ or D/H) of vapour in the cloud and R_V the ratio after a given proportion of the vapour has rained out to yield the precipitation with the isotopic ratio R_l from liquid equilibrium value (R_{l0}) corresponding to R_{V0}. The residual fraction in vapour reservoir is denoted by 'f'. The factor 'α' denotes the equilibrium water→vapour fractionation factor at the prevailing *in-cloud* temperature.

Along the trajectory, when part of the rained out vapour is returned to the atmosphere by means of evapotranspiration, this simple Rayleigh law, however, is not applicable. The downwind effect of the evapotranspiration flux on the isotopic composition of the atmospheric vapour and precipitation depends on the details of the evapotranspiration process. Transpiration returns precipitated water essentially un-fractionated back to the atmosphere, despite the complex fractionation in leaf water (Zimmermann et al, 1967; Forstel, 1982). Thus transpiration, by returning vapour mass with isotopic composition R_V (= R_l/α) in the downwind direction, in a way restores both the vapour mass and the heavy isotope depletion caused by the rainout in such a way that the next rainout event is not as depleted as it would have been without the

transpiration flux. Under such circumstances, the change in the isotopic composition along the air mass trajectory is only due to the fraction 'f_{net}', representing the net loss of water from the air mass, rather than being a measure of the integrated total rainout. This causes apparent reduction in the downwind isotopic gradient. The evaporated water, on the other hand, is usually depleted in heavy species relative to that of transpired vapour (i.e $<R_V$), thus restoring the vapour mass to the downwind cloud but reducing its isotopic composition. This causes apparent increase in the downwind isotopic gradient.

The isotopic imprints of evaporation are also recorded in the form of a parameter *d*-excess (discussed below), in the evaporating water body, the evaporated vapour and the precipitation from the admixture of atmospheric vapour and the evaporated flux. Since the kinetic fractionation for ^{18}O is more than that for D, as seen from Eq. (2.5) and Eq. (2.6), the relative enrichment of the residual water for an evaporating water body is more for ^{18}O than for D. Correspondingly, for the resulting vapour the depletion is more for ^{18}O than for D. The extent to which ^{18}O is more fractionated compared to D can be represented by a parameter *d*-excess defined by Dansgaard (1964) as below:

$$d\text{-excess} = d = \delta D - 8 \times \delta^{18}O \quad (‰)$$

Eq. (2.11)

The *d*-excess as defined above represents the excess δD than 8 times $\delta^{18}O$ for any water body or vapour. Since magnitude of equilibrium fractionation for D is about 8 times that for ^{18}O, any value of δD in vapour, in excess of 8 times $\delta^{18}O$ signifies the effect of kinetic fractionation due to evaporation. As mentioned earlier, the intercept (~10‰) of GMWL also signifies the kinetic fractionation during evaporation but the difference between intercept and *d*-excess is that the intercept of a meteoric or any other water line is valid for an entire dataset whereas, the *d*-excess parameter can be calculated for a single water sample whose δD and $\delta^{18}O$ values are known.

As the evaporation proceeds, because of relatively higher enrichment of ^{18}O in the residual water, the *d*-excess of the evaporating water body decreases and that of the resulting vapour increases. Therefore, if the original water was meteoric in origin, the residual water not only gets enriched in heavier isotopes but also shows progressively lower *d*-excess values as the evaporation proceeds i.e. its position on the $\delta^{18}O - \delta D$ plot will be below the Local Meteoric Water Line. The resulting vapour on the other hand shows the opposite effect. Further, since condensation and consequentially rainout is an equilibrium process (with slope ~8), it does not significantly alter the *d*-excess. Thus, *d*-excess provides an additional handle on identifying vapours of different histories and their mixing. Due to the effect of evaporation, most meteoric and subsurface processes

shift the $\delta^{18}O$–δD signatures of water to a position below the LMWL. It is rare to find precipitation or groundwaters that plot above the LMWL, i.e., showing higher *d*-excess. However, in low-humidity regions, re-evaporation of precipitation from local surface waters and/or soil water/ water table creates vapour masses with isotopic content that plots above the LMWL. If such vapours are re-condensed in any significant quantity before mixing with the larger tropospheric reservoir, the resulting rainwater will also plot above LMWL (Clark and Fritz, 1997), along a condensation line with slope ~8. It is however, important to recall that recycling of water back to the atmosphere in the form of vapour from soil moisture by plant transpiration is a non-fractionating process that does not affect the *d*-excess.

A small fraction of rain percolates down through the soil layer eventually to become groundwater. For many ground waters, their isotopic composition has been shown to equal the mean weighted annual composition of precipitation (Krishnamurty and Bhattacharya, 1991; Bhattacharya et al, 1985; Hamid et al, 1989; Douglas, 1997; Rank et al, 1992). However, significant deviations from precipitation are also found in several cases. Such deviations from local precipitation are more pronounced in arid zones due to extensive evaporation from the unsaturated zone or even evaporative losses from water table (Dincer et al, 1974; Allison et al, 1983). Considering that only a small percentage of precipitation actually reaches the water table in most situations, the meteoric signal in ground water can get significantly modified. Isotope variations in precipitations get attenuated and seasonal biases in recharge are imparted to the newly formed ground water. This bifurcation of the hydrological cycle between precipitation and surface water on one hand and groundwater on the other ends where groundwater discharges and rejoins surface runoff in streams and rivers. Environmental isotopes play a significant role in quantifying relative contribution of groundwater to stream flow and in understanding the hydraulic processes operating in a catchment area.

2.5 Chlorofluorocarbons

Chlorofluorocarbons (CFCs) are non-flammable, non-corrosive, non-explosive, non-carcinogenic, very low toxic and stable halogenated alkanes synthesised first in early 1930s as safe alternatives to ammonia and sulphur dioxide in refrigeration and air-conditioning. Because of such peculiar physical properties, CFCs are suitable for a wide range of industrial applications such as blowing agents in foams, insulation, packing materials, propellants in aerosol cans solvents, in vapour degreasing and cold immersion cleaning of microelectronic components and in surface cleaning procedure. There are several CFC compounds produced commercially for industrial applications but the three

most important CFC species that provide as excellent hydrological tracers are Trichloro-fluoromethane (CFC-11 or F-11), Dichloro-difluoromethane (CFC-12 or F-12) and Trichloro-trifluoroethane (CFC-113 or F-113) (Busenberg and Plummer, 1992; Dunkle et al, 1993; Cook and Solomon, 1995, 1997). The basic fact sheet of these compounds, is given in Table 2.5 which is compiled from Volk et al, 1997; Plummer and Busenberg, 1999 and Busenberg and Plummer, 1992.

Table 2.5 The basic fact sheet of important CFC species.

	CFC-11	**CFC-12**	**CFC-113**
Produced since (year)	1936	1931	1945
Name	Trichloro-fluromethane	Dichloro-difuoromethane	Trichloro-trifluoroethane
Formula	$CFCl_3$	CF_2Cl_2	$C_2F_3Cl_3$
Molecular Wt. (g/mol)	137.5	121	187.5
Boiling Point	24 ^{0}C	–29 ^{0}C	48 ^{0}C
Air mixing ratios (pptv)	249.6 pptv (NH) 247.8 pptv (SH)	538.7 pptv (NH) 538.6 pptv (SH)	78.1 pptv (NH) 78.0 pptv (SH)
Atmospheric life time	45 ± 7 years	87 ± 17 years	100 ± 32 years
(NH) = Northern Hemisphere; (SH) = Southern Hemisphere;			

The atmospheric build up of CFCs in southern and northern hemispheres is shown in Figure 2.4 It is seen that atmospheric concentration of CFCs rose rapidly through the 1970s and 1980s. This observation is in accordance with the fact that annual production of CFC-11 and CFC-12 peaked in 1987 and that of CFC-113 peaked in 1989 (AFEAS, 1997). With the realisation that CFCs are a prime contributor to stratospheric ozone depletion, Montreal Protocol (1987) on "Substances that Deplete the Ozone Layer" was signed by 37 nations which agreed to limit the release of CFCs and to reduce the CFC emissions to 50% by the year 2000. In 1990, this protocol was strengthened, requiring industrial countries to completely phase out CFCs by the year 2000, and developing countries by 2010. The Protocol received a major boost in 1992 when 90 countries agreed to cut off the production of CFCs by 1996. With various degrees of compliance with these agreements, the atmospheric concentration of CFCs started falling. As seen in Figure 2.4, air mixing ratios of CFC-11 and CFC-113 peaked around 1993 and 1994 respectively. Elkins et al. (1993) have reported peak values of 275.1 and 85.4 pptv respectively for CFC-11 and CFC-113, in North America. The air mixing ratio of CFC-12 is seen to peak in year 2003 and declines slowly thereafter.

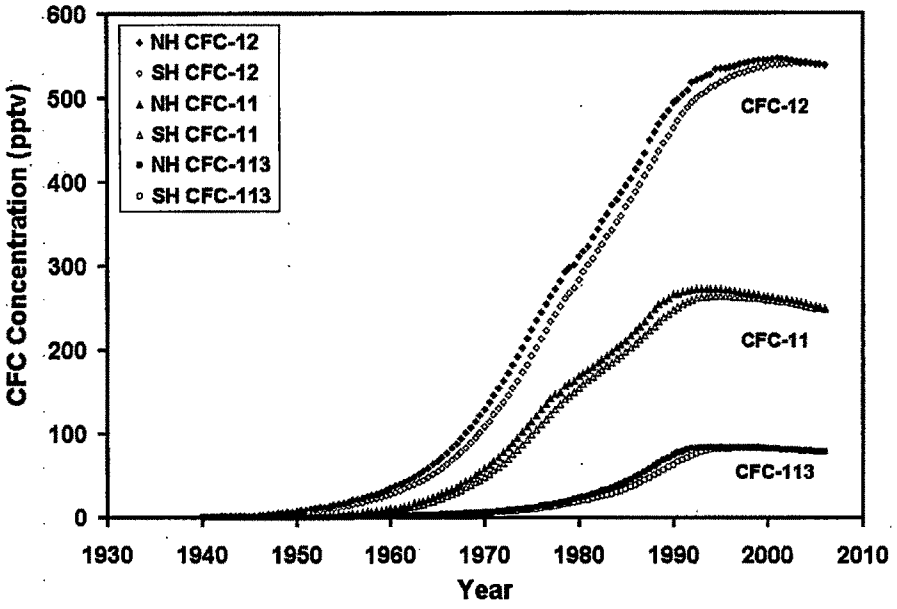

Figure 2.4 Atmospheric mixing ratios of CFC-11, CFC-12 and CFC-113 for Northern and Southern Hemisphere (NH and SH) atmosphere. Redrawn from United States Geological Survey (URL: http://water.usgs.gov/lab/software/air_curve/).

Atmospheric concentrations of CFC-11, -12 and -113 increased up to the minimum detection levels from about 1941, 1947 and 1955 respectively. CFCs dissolve in water in equilibrium with atmospheric air proportional to their mixing ratios and are subsequently carried underground by infiltrating water. Therefore, by measuring concentrations of CFC-11, CFC-12 and CFC-113, it is possible to identify groundwater recharged since about 1941, 1947 and 1955. The possibility of employing CFCs as tracers of recent recharge and indicators of groundwater age was first recognised in the 1970s (Thompson et al, 1974; Schults et al, 1976; Randall and Schultz, 1976). The progressive development in applicability of CFCs as hydrological tracers since 1970s has been described by Plummer and Busenberg (1999).

After isolation from the unsaturated zone and the soil atmosphere, newly recharged water may carry dissolved CFCs, into the aquifer. Thus, the CFC concentrations in groundwater at any location can, in principle, be traced back to atmospheric partial pressure of CFCs at the time of recharge. Therefore, the time elapsed since the groundwater lost contact with the atmosphere can be estimated. However, there may be exchange between gases dissolved in equilibrium with atmosphere and gases in the unsaturated zone invalidating the inherent assumption of no addition or removal of CFCs to or from the recharged water.

The isolation of a parcel of water from the unsaturated zone air is a function of several factors including (i) recharge rate; (ii) porosity of the unsaturated zone; (iii) aqueous and gaseous diffusion coefficients; and (iv) magnitude of water table fluctuation. There is evidence of loss of dissolved gases such as ^{3}He during vertical transport of water (Schlosser et al, 1989; Solomon et al, 1993). However, Cook and Solomon (1997) pointed out that CFCs have higher solubility and lower diffusion coefficients than ^{3}He. An investigation of CFC concentration in air and shallow groundwater revealed that groundwater during seasonal water table low preserved the CFC concentration formed when water table was near land surface and in equilibrium with atmosphere (Cook et al, 1995). Further, the molecular diffusion coefficients of gases in water are some 5 orders of magnitude smaller than in air. Thus, despite possibility of molecular diffusion, the shallow groundwater remains closed to gas exchange and CFC confinement is thought to occur fairly rapidly (Cook and Solomon, 1997).

The CFC concentrations can also be affected by various physical and chemical processes such as degradation and sorption during transit within the unsaturated zone and the soil zone. Soil-gas CFCs concentrations and the ratio of CFC-11 to CFC-12 are reported to decrease with depth indicating that various dissolved CFCs can be unequally retarded during their downward movement in unsaturated zone depending on tortuosity, sorption and dissolution in pore water (Weeks et al, 1982; Khalil and Rasmusen, 1989; Brown, 1980). These studies also indicate that CFCs are absorbed by soils in a magnitude decreasing with increasing fluorine content. The magnitude of absorption is dependent on the organic content of soil and is independent of mineralogy. The CFCs absorbed by dry soils can be subsequently released when soils become wet again.

The dissolved CFC concentration can also be modified by microbial degradation particularly in an anoxic environment. There is experimental evidence of microbial degradation of CFCs mainly after completion of denitrification reactions which indicate that microbial population other than denitrifiers are responsible for degradation of CFCs and rate of biodegradation is inversely related to fluorine content of halocarbons (Semprini et al, 1990). The microbial degradation, however, is not observed in the oxic environments. Additional CFCs, over and above atmospheric equilibration value, can also be introduced into groundwater due to entrapment and subsequent dissolution of air bubbles (See section 2.1), similar to that for helium (Heaton, 1981; Heaton and Vogel, 1981; Andrews et al, 1985).

Despite various factors that may give rise to uncertainties in the interpretation, CFCs in groundwater have been used advantageously to (i) identify the recent recharge;

(ii) estimate the time of recharge; and also (iii) explain differences in apparent ages in an aquifer (Busenberg and Plummer, 1992; Dunkle et al, 1993).

Over the last three decades there has been advancement in the analytical techniques, sampling and storage procedure and reliability and adequacy of data such as reconstructed atmospheric mixing ratios, Henry's solubility constants etc (Plummer and Busenberg, 1999). As a result, CFCs are now increasingly employed as tracers for studying oceanic circulation, ventilation and mixing, unsaturated zone processes and for identifying recent recharge and dating of young (~50 years time scale) ground waters (Plummer and Busenberg, 1999). It must, however, be stated that analyses of CFCs in water still remains quite tricky and cumbersome. Therefore, there are only a few functional laboratories in the world to measure dissolved CFCs.

2.6 Groundwater Dating

In an aquifer system, ensemble of water molecules arriving at a particular location within the aquifer comprises molecules that spend various time durations between recharge and their reaching a particular location. The concept of groundwater dating involves estimating the average time spent by the molecules before reaching a given location. The age of groundwater at a particular location is the estimated average time spent by the water molecules in the aquifer since the time of recharge and before arriving at that location. Depending on the conceptual mathematical model of the aquifer system, the age can give different additional information about the aquifer system. The various conceptual models in common use are: (i) the Piston Flow Model (PFM); (ii) the Well-Mixed Reservoir Model (WMRM); and (iii) the Dispersion-Advection Model (DAM).

The most commonly used groundwater flow model for estimating groundwater age assumes that as groundwater moves away from the recharge area, there are no flow lines of different velocities and that hydrodynamic dispersion as well as molecular diffusion of water molecules are negligible. Thus, water moves from the recharge area very much like a parcel pushed by a piston with mean velocity of groundwater (Piston Flow Model; PFM). This implies that a radiotracer which appears at the sampling point at any time "t" has entered the system at a time "t-T", and from that moment its concentration has decreased by radioactive decay during the time span "T" spent in the aquifer. Therefore:

$$C_{out}(t) = C_{in}(t-T) \,.\, \exp(-\lambda T)$$

Eq. (2.12)

This equation describes a dynamic system and is mathematically equivalent to describing the concentration of a radioisotope in a static water parcel separated since its recharge, whereby:

$$C_t = C_0 \,.\, \exp(-\lambda T)$$

Eq. (2.13)

Here, "t" is the radiometric age of the water and corresponds to "T" of the dynamic system. If "x" is the distance from the recharge boundary, T = x/u can be used to estimate the flow rate (u) of groundwater in the aquifer.

$$C_t = C_0 \exp(-\lambda x/u)$$

Eq. (2.14)

Unlike in the PFM, if it is assumed that the recharge flux completely mixes with the entire volume of the reservoir before outflow, we get another extreme situation and the model is known as Well Mixed Reservoir (WMR) model. In applying this model to an aquifer system, it is assumed that the well-mixed reservoir comprises the entire volume between the recharge area and the sampling point. Under this condition for a radiotracer,

$$C_t = C_0 / (1+\lambda\tau)$$

Eq. (2.15)

In Eq. (2.15), "λ" is the radioactive decay constant and "τ" is the ratio of the reservoir volume to the flux into the reservoir and represents the estimated mixing time (or the mean residence time) between the recharge area and the sampling location. It is seen that τ estimated from the tracer data actually represents a dynamic parameter – the mixing time.

$$\tau = \frac{1}{\lambda}\left(\frac{C_0}{C_t} - 1\right)$$

Eq. (2.16)

The phenomenon of mixing accompanying the movement of water molecules through porous media can also be described by a diffusion-advection equation in which the diffusion coefficient is replaced by a dispersion coefficient (Scheidegger, 1961; Gupta, 2001). For a radiotracer, the one dimensional continuity equation in groundwater flow system may be written as (Guymon,1972):

$$\frac{\delta C}{\delta t} = \frac{\delta\left(D\,\delta C/\delta x - uC\right)}{\delta x} + W_1 - W_2$$

Eq. (2.17)

In the above equation, "D" is the diffusion coefficient of the tracer, and as in the case of PMF, "x" is the distance from the recharge boundary, "u" is the bulk flow velocity, "W_1" and "W_2" are the rates of the introduction and removal of the tracer respectively. With further assumptions of u and D not being function of x and in case of steady state (i.e. dC/dt = 0), the above equation reduces to:

$$D\frac{\partial^2 C}{\partial x^2} - u\frac{\partial C}{\partial x} W_1 - W_2 = 0$$

Eq. (2.18)

In case of radioactive tracers, the term W_2 will include, in addition to radioactive decay, loss of tracer from water due to non-radioactive processes (e.g. adsorption on the aquifer matrix). Dealing with the case of loss of tracer by radioactive decay alone and for $W_1 = 0$, the above equation can be rewritten as:

$$D\frac{\partial^2 C}{\partial x^2} - u\frac{\partial C}{\partial x} - \lambda C = 0$$

Eq. (2.19)

This equation for the case of D = 0, and the boundary condition $C = C_0$ at x = 0 give the solution for the piston flow Eq. (2.14).

In case of finite dispersion, the solution of Eq. (2.19) for the boundary conditions $C = C_0$ at x = 0 and C = 0 at ∞, is given by Gupta et al (1981).

$$C/C_0 = \exp\left[\frac{xu}{2D}\left\{1-\left(1+4\lambda D/u_2\right)^{1/2}\right\}\right]$$

Eq. (2.20)

The tracer concentration decreases exponentially with distance similar to the case of PFM. Therefore, a simplistic application of the PFM would give an apparent velocity:

$$u_a = \frac{u}{2}\left\{1-\left(1+4\lambda D/u^2\right)^{1/2}\right\}$$

Eq. (2.21)

There are several other mathematical models in use that conceptualize the flow of groundwater in aquifer system differently depending on specific understanding of the geometry, and flow paths. But for confined aquifers with a definite recharge area, the above models are most frequently used to interpret the environmental isotopic data and

to determine the groundwater age evolution from recharge to discharge regions. This, though, is still a challenging task for hydro-geochemists because sampling locations are often randomly distributed over an area where water from an aquifer is pumped from various depths or where springs bring water to the surface. Several environmental tracers (including radio nuclides) find application in determining direction and magnitude of groundwater flow, hydro-geological parameters of the aquifer and age of groundwater (Andrews et al., 1989; Cserepes and Lenkey, 1999).

In regional aquifer systems, groundwater ages may range up to 10^3 ka and more. Radiocarbon, with half-life ($t_{1/2}$) of 5.73 ka, can be used for groundwater dating up to ~35 ka (Geyh, 1990). The other available radio nuclides such as ^{36}Cl ($t_{1/2}$ = 3.01x 10^2 ka; Andrews and Fontes, 1992), ^{81}Kr ($t_{1/2}$ = 2.1x10^3 ka; Lehmann et al., 1991) and ^{234}U ($t_{1/2}$ = 2.45x10^2 ka; Fröhlich and Gellermann, 1987) enable groundwater age determination well beyond the radiocarbon dating range. On the other hand, the range of groundwater ages that can be estimated by radiogenic ^4He is 1–100 ka (Torgersen, 1980; 1992; Mazor and Bosch, 1992; Clark et al., 1998; Castro et al., 2000). When combined with ^{222}Rn activity measurements, the $^4He/^{222}Rn$ systematics also provides estimation of groundwater age in the range 1–1000 ka (Torgersen, 1980; Gupta et al, 2002). Another advantage of both ^4He and $^4He/^{222}Rn$ methods is that measurements of ^4He and ^{222}Rn are relatively simple. However, some complications also exist.

2.6.1 ^{14}C Dating Method

The radiocarbon (^{14}C) dating method for groundwater is based on measuring the residual activity of ^{14}C, in total dissolved inorganic carbon (TDIC) of a given groundwater sample. The groundwater age is estimated using:

$$\text{Age}(t) = -\frac{1}{\lambda_{14}} \cdot \ln\left(\frac{A_t}{A_0}\right)$$

Eq. (2.22)

In Eq. (2.22), ^{14}C activities are expressed in terms of percent modern carbon (pmC). The activity of 'modern Carbon' is defined as 95% of the ^{14}C activity in 1950 of the NBS oxalic acid standard. This is close to the activity of wood grown in 1890 in a fossil-CO_2-free environment and equals 13.56 dpm/g carbon. Thus, expressed in pmC, A_t refers to ^{14}C activity of TDIC in groundwater at the time of sampling and A_0 the initial activity in the recharge area; λ_{14} is the radioactive decay constant for ^{14}C and t is the estimated age.

Two key assumptions made in this method are: (i) A_0 is known and has remained constant in time; and (ii) the system is closed to subsequent gain or loss of the parent, except by the radioactive decay. In the case of radiocarbon dating of vegetal remains, A_0 can be taken as equal to 100 pmC since the only source of ^{14}C is atmospheric CO_2. However, in the case of ground waters, A_0 in TDIC depends on contribution from soil CO_2 and from soil carbonates which can have any value of ^{14}C activity between zero (radioactively dead carbon) to 100 pmC. Depending on the contribution from soil carbonates, A_0 can have any value between 50–100 pmC. This is because, of the two carbon atoms in the molecule of $Ca(HCO_3)_2$ in TDIC, [$CaCO_3 + H_2O + CO_2 \leftrightarrow Ca(HCO_3)_2$], one is derived from soil CO_2 and the other from soil carbonate. There is further complication due to isotopic exchange between TDIC and the soil CO_2 and carbonate material. There are several models that attempt to estimate the contribution of soil carbonates to the TDIC and estimate the applicable value of A_0. This is done either through a stoichiometry approach for the various chemical reactions involving carbon or by estimating dilution of active carbon using an isotope mixing approach based on ^{13}C content of each species involved or a combination of the two approaches. Various methods for estimating A_0 can be found in Mook (1976) and Fontes and Garnier (1979). The error due to incorrect estimation of A_0, however, is $<t_{½}$ of ^{14}C, except in some special case of carbonate aquifers where continuous exchange between TDIC and the aquifer matrix may reduce A_0 to <50 pmC. Since most of the chemical and isotope exchange occurs in the unsaturated soil zone during the process of groundwater recharge, and between TDIC and the soil CO_2, the A_0 in several ground waters has been found to be 85±5 pmC (Vogel, 1967; 1970).

In the present investigation, the theoretical value of A_0 after equilibrium between soil CO_2, soil carbonate (at ^{14}C = 0 pmC; $\delta^{13}C$ = 0‰) and infiltrating water has been achieved, is estimated using the following equation (Münnich, 1957; 1968):

$$A_0 = \frac{\delta^{13}C_{TDIC}}{\delta^{13}C_{soil} - \varepsilon} 100$$

Eq. (2.23)

Where, $\delta^{13}C_{TDIC}$ is the $\delta^{13}C$ value of the groundwater TDIC, $\delta^{13}C_{soil}$ is the $\delta^{13}C$ of soil CO_2 (~–22‰) and ε is equilibrium fractionation between the soil CO_2 and the TDIC of groundwater (~–9‰). This is done with the knowledge that application of any other model would give radiocarbon ages differing by < ± 2ka. Also because, in regional aquifers, the difference in groundwater ages between any two locations, after the

confinement of the groundwater in the aquifer becomes effective, depends little on the applicable value of A_0.

2.6.2 ^{4}He Dating Method

The Helium-4 dating method for groundwater is based on estimating the amount and rate of accumulation of *in situ* produced radiogenic ^{4}He in groundwater (Andrews and Lee, 1979; Stute et al, 1992a). If secular equilibrium and release of all the produced ^{4}He atoms in the interstitial water are assumed, the groundwater ages can be calculated from the annual ^{4}He production rate estimated as (Torgersen, 1980):

$$J'_{He} = 0.2355 \times 10^{-12} U^* \qquad \text{Eq. (2.24)}$$

where,

$$U^* = [U]\{1+0.123([Th]/[U] - 4)\} \qquad \text{Eq. (2.25)}$$

J'_{He} = production rate of ^{4}He in cm^3 STP g^{-1} rock a^{-1}; [U] and [Th] are concentrations (in ppm) of U and Th respectively in the rock/sediment.

Accumulation rate (AC'_{He}) of ^{4}He in cm^3 STP cm^{-3} water a^{-1} is therefore, given by:

$$AC'_{He} = J'_{He}.\rho.\Lambda_{He}.(1-n)/n \qquad \text{Eq. (2.26)}$$

Where, Λ_{He} = helium release factor; ρ = rock density (g cm^{-3}); n = rock porosity.

Since the helium measurements were actually made on equilibrated headspace air samples, in the present study, the dissolved helium concentrations (cm^3 STP cm^{-3} water) are expressed in terms of Air Equilibration Units (AEU) which expresses the dissolve helium in terms of the corresponding equilibrium dry gas phase mixing ratio at 1 atmospheric pressure and 25°C. As a result, water in equilibrium with air containing 5.3 ppmv helium is assigned dissolved concentration of 5.3 ppmAEU. Water of meteoric origin will have a minimum helium concentration ($^4He_{eq}$) of 5.3 ppmAEU, acquired during its equilibration with the atmosphere. Excess helium ($^4He_{ex}$) represents additional helium acquired by groundwater either from *in situ* produced radiogenic ^{4}He or any other subsurface source.

Using a dimensionless Henry Coefficient (H_x) of 105.7 for helium at 25°C (Weiss, 1971), 5.3 ppmAEU corresponds to a moist air equilibrium concentration of 4.45×10^{-8} cm^3 STP He. cm^{-3} water. Therefore,

$$AC_{He} = AC'_{He} . 10^6 . H_X . (T/T_0) . P_0 / (P_0 - e)$$

Eq. (2.27)

where, AC_{He} = accumulation rate of ^4He in ppmAEU a^{-1}; T_0 = 273.15° K; P_0 = 1 atm and e = saturation water vapour pressure (0.031 atm) at 25°C, H_x = 105.7.

For an average [U] = 1 ppm for alluvial sedimentary formations and [Th]/[U] = 4 (Ivanovich, 1992), n = 20 %; Λ_{He} = 1; ρ = 2.6 g cm^{-3}, *in situ* ^4He accumulation rate (AC_{He}) of 2.59×10^{-4} ppmAEU a^{-1} is obtained. Therefore, from the measured helium concentration of the sample (^4He_s), the age of groundwater can be obtained by using:

$$\text{Age (t)} = {}^4He_{ex} / AC_{He}$$

Eq. (2.28)

where, $^4He_{ex}$ is obtained by subtracting $^4He_{eq}$ (= 5.3 ppmAEU at 25°C and 1 atmospheric pressure) from the measured concentration in groundwater sample (^4He_s).

The above formulae, however, ignores 'excess air' helium ($^4He_{ea}$) due to supersaturation of atmospheric air as the groundwater infiltrates through the unsaturated zone. Various models have been proposed for estimating this component in groundwater studies (Aeschbach–Hertig et al., 2000; Kulongoski et al., 2003) based on measurement of other dissolved noble gases. Since measurement of dissolved noble gases has not been made in this study, it has not been possible to correct for this effect. However, from other studies (Holocher et al., 2002) it appears that $^4He_{ea}$ can be up to 10–30% of $^4He_{eq}$ giving a possible overestimation of groundwater age up to ~ 6 ka.

Further, (^4He_s) can contain other terrigenic helium components (Stute et al., 1992a) that can cause overestimation of groundwater age. These terrigenic components are: (i) flux from an external source e.g. deep mantle or crust, adjacent aquifers etc. (Torgersen and Clarke, 1985); and (ii) release of geologically stored ^4He from young sediments (Solomon et al., 1996). Depending upon the geological setting, particularly in regions of active tectonism and/or hydrothermal circulation, the contribution of these sources may exceed the *in situ* production by several orders of magnitude (Stute et al., 1992a; Minissale et al., 2000; Gupta and Deshpande, 2003a). Additional measurements/ data (e.g. $^3He/^4He$, other noble gases) are required to resolve these components. For recent reviews on terrigenic helium, reference is made to Ballentine and Burnard (2002) and Castro et al. (2000). However, in many cases it seems possible to rule out major

contribution from terrigenic He sources since the helium flux may be shielded by underlying aquifers that flush the Helium out of the system before it migrates across them (Torgersen and Ivey, 1985; Castro et al., 2000). According to Andrews and Lee (1979), with the exception of a few localised sites and for very old ground waters, 'excess He' in groundwater is due to *in situ* production only and is often used for quantitative age estimation within the aquifer if the U and Th concentrations of the aquifer material are known. But, in case, there is evidence of deep crustal ^4He flux (J_0) entering the aquifer, the Eq. (2.28 gets modified to (Kulongoski et al, 2003):

$$Age(t) = {}^4He_{Ex} / [(J_0 / n Z_0 \rho_w) + AC_{He}] / 8.39 \times 10^{-9}$$

Eq. (2.29)

where, Z_0 is the depth (m) at which the ^4He flux enters the aquifer and ρ_w is the density of water (1 g cm^{-3}).

2.6.3 $^4He/^{222}Rn$ Dating Method

Since both ^4He and ^{222}Rn have a common origin in groundwater, being produced by the α decay of U and/or Th in the aquifer material, their simultaneous measurements in groundwater can also be utilized for calculating its age (Torgersen, 1980).

As in case of ^4He, the ^{222}Rn accumulation rate (AC_{Rn}) in cm^3 STP cm^{-3} water a^{-1} is given by:

$$AC_{Rn} = J'_{Rn} . \rho . \Lambda_{Rn} . (1-n)/n$$

Eq. (2.30)

$$\text{where, } J'_{Rn} = 1.45 \times 10^{-14} [U]$$

Eq. (2.31)

and J'_{Rn} = production rate of ^{222}Rn in cm^3 STP g^{-1} rock a^{-1} and [U] = concentration (in ppm) of U in the rock/sediment.

Thus, computing accumulation rate ratio of ^4He and ^{222}Rn (= AC_{He}/AC_{Rn}), the age of groundwater can be calculated as follows:

$$Age(t) = (\Lambda_{Rn}/\Lambda_{He})(AC_{Rn}/AC_{He})(C_4/A_{222})$$

Eq. (2.32)

where, $\Lambda_{Rn}/\Lambda_{He}$ is the release factor ratio for radon and helium from the aquifer material to groundwater; C_4 is concentration (atoms l^{-1}) of ^4He and A_{222} is activity (disintegration l^{-1} a^{-1}) of ^{222}Rn in groundwater. From Eq. (2.24) to Eq. (2.26) and Eq. (2.30) to Eq. (2.32) it is seen that $^4He/^{222}Rn$ ages are independent of porosity, density

and U concentration, but do require a measure of [Th]/[U] in the aquifer material. The ratio $\Lambda_{Rn}/\Lambda_{He}$ depends upon grain size and recoil path length of both ^{222}Rn (~0.05μm) and ^{4}He (30–100μm) (Andrews, 1977). Release of ^{222}Rn by α–recoil from the outer surface (~0.05μm) of grain (~2–3mm) has been estimated to be ~0.005% (Krishnaswami and Seidemann, 1988). Apart from α–recoil, both ^{222}Rn and ^{4}He can diffuse out from rocks/ minerals through a network of 100–200Å wide nanopores throughout the rock or grain body (Rama and Moore, 1984). Radon release factor (Λ_{Rn}) ranging from 0.01–0.2 has been indicated from laboratory experiments for granites and common rock forming minerals (Krishnaswami and Seidemann, 1988; Rama and Moore, 1984). On the other hand, Torgersen and Clarke (1985), in agreement with numerous other authors, have shown that most likely value of $\Lambda_{He} \approx 1$. Converting C_4 (atoms l^{-1}) to C_{He} (ppmAEU) units and A_{222} (disintegration l^{-1} a^{-1}) to A'222 (dpm l^{-1}) units, Eq. (2.32) can be rewritten as:

$$\text{Age (t)} = 4.3\text{x}10^{6}\cdot(\Lambda_{Rn}/\Lambda_{He})\cdot(AC_{Rn}/AC_{He})\cdot C_{He}\ /A'_{222} \qquad \text{Eq. (2.33)}$$

Here, 1 ppmAEU ^{4}He concentration corresponds to 2.26 x 10^{14} atoms of ^{4}He l^{-1} of water. Another inherent assumption of $^{4}He/^{222}Rn$ dating method is that both ^{4}He and ^{222}Rn originate from the same set of parent grains/rocks and their mobilization in groundwater is similarly affected.

Andrews et al. (1982) used following one–dimensional equation for calculating diffusive transport of ^{222}Rn in granites:

$$C_x = C_0 \exp(-\sqrt{\lambda/D}.X) \qquad \text{Eq. (2.34)}$$

where, C_0 and C_x are concentration of ^{222}Rn from an arbitrary x = 0 and at x = x respectively; D = diffusion coefficient in water (~10^{-5} cm^2 s^{-1}); and λ = decay constant for ^{222}Rn. They calculated that $C_x/C_0 = 0.35$ at a distance equal to one diffusion length (X = $[D/\lambda]^{1/2}$ i.e. 2.18 cm). Therefore, even at high ^{222}Rn activity its diffusion beyond few metres distance is not possible. The average radon diffusion co–efficient in soils with low moisture content and composed of silty and clayey sand is even lower ~$2\text{x}10^{-6}$ cm^2 s^{-1} (Nazaroff et al., 1988). Therefore, ^{222}Rn measurements of groundwater depend essentially on U in the pumped aquifer horizons in the vicinity of the sampled tubewell.

Therefore, for ground waters that may have a component external to the aquifer, the measured ^{222}Rn because of its short half–life ($t_{1/2}$ = 3.825 d) is indicative of local mobilisation only. Whereas ^{4}He, being stable, might have been mobilized from the entire

flow–path. In such cases, the resulting $^{4}He/^{222}Rn$ ages for groundwater samples having high 'excess He' might be over estimated.

2.6.4 CFC Dating Method

Groundwater dating with CFCs is possible because: (i) the atmospheric mixing ratios of CFCs are known or have been reconstructed over the past 50 year; (ii) the Henry's law solubility of CFCs in water are known; and (iii) technology to measure low concentrations of CFCs in water has been developed. CFC age of groundwater actually estimates the time since the water became isolated from the air in unsaturated zone. However, in view of possibility of modifications of dissolved CFC concentration during transit, it is more appropriate to use the term 'CFC-model age' or 'CFC-apparent age'. The basic assumption in assigning the model age is the piston flow model (PFM; See Section 2.6 above). The inferred model age assumes that the concentration of the CFC was not altered by the transport processes from the point of entry to the measurement point in the aquifer. Most of the apparent CFC ages referred to in the literature are based on PFM (Plummer and Busenberg, 1999).

The scope of the present work is limited to setting up of the groundwater CFC laboratory at PRL for future application. Therefore, further details including the mathematics involved in groundwater dating with CFCs are not presented here.

In Chapter 3 next, details of the field and laboratory procedures for sample collection, storage, instrument calibration and analyses using CFC standard are described. Also described in Chapter 3 are similar details for other tracer techniques used in this study.